Ceramide, a target for antiretroviral therapy

Catherine M. Finnegan*, Satinder S. Rawat*, Anu Puri*, Ji Ming Wang†, Francis W. Ruscetti‡, and Robert Blumenthal*§

Laboratories of *Experimental and Computational Biology, †Molecular Immunoregulation, and ‡Experimental Immunology, Center for Cancer Research, National Cancer Institute, National Institutes of Health, Frederick, MD 21702

Edited by Robert C. Gallo, University of Maryland Biotechnology Institute, Baltimore, MD, and approved September 14, 2004 (received for review April 23, 2004)

Studies of ceramide metabolism and function in a wide range of biological processes have revealed a role for this lipid in regulating key cellular responses. Our research on the role of sphingolipids in HIV entry has led to the hypothesis that modulation of ceramide levels in target cells affects their susceptibility to HIV infection by rearranging HIV receptors. Cellular ceramide levels were modulated by application of pharmacological agents such as *N*-(4-hydroxyphenyl)retinamide (4-HPR, fenretinide), by treatment with sphingomyelinase (Smase), or by exogenous addition of long-chain ceramide, and determined after metabolic incorporation of [^{3}H]sphingosine. Infectivity assays were performed by using a HeLa-derived indicator cell line, TZM-bl, CD4$^+$ lymphocytes, and monocytes. We observed a dose-dependent inhibition by 4-HPR of infection of TZM-bl cells by a broad range of HIV-1 isolates at low micromolar concentrations with an IC_{50} of <1 μM for most isolates tested. Nearly complete inhibition was seen at 5 μM, a dose that enhanced ceramide levels by 50–100%, yet was nontoxic to the cells. Treating cells with other pharmacological agents that enhanced ceramide levels, with Smase, or exogenous addition of long-chain ceramide also resulted in inhibition of HIV-1 infection. Enhancing ceramide levels in CD4$^+$ lymphocytes and in monocyte-derived macrophages with 4-HPR or Smase significantly reduced infectivity without toxicity. The minimal toxicity of normal cells exposed to 4-HPR should make the drug exceedingly suitable as an anti-HIV therapeutic.

HIV entry is mediated by the sequential interaction of the viral envelope protein with CD4 and a chemokine receptor on the target cell (1). Several lines of evidence indicate that these interactions occur at distinct domains on the target-cell membrane (2). The integrity of membrane domains is critical for viral entry because disruption of domain structure upon modulation of cellular cholesterol or glycosphingolipid levels results in inhibition of HIV infection (3).

Ceramide, a derivative of the lipid sphingosine, has been implicated in regulating a diverse array of events, including differentiation, senescence, cell-cycle arrest, proliferation, and apoptosis (4). Such effects have been attributed to the second messenger signaling capabilities of this lipid, which are facilitated by its biophysical properties. With a small hydroxy head group and two long saturated hydrophobic chains, in addition to intermolecular hydrogen bonding, ceramide packs tightly in bilayers and promotes membrane rigidity. Ceramide plays an important role in organizing membrane structure because it has a tendency to self-aggregate and segregate into membrane microdomains (5). Increasing ceramide concentrations has been implicated in modulation of endocytic pathways, vesicle aggregation, enhanced membrane permeabilization, and induction of lipid microdomain formation (6).

Because membrane organization is critical for HIV infection, we investigated the role of ceramide in the entry of this neutral pH-fusing virus. To this end, we stimulated *de novo* ceramide biosynthesis through pharmacological manipulation and directly increased plasma membrane ceramide levels through addition of exogenous ceramide and through enzymatic cleavage of sphingomyelin at the plasma membrane. We report that the accumulation of ceramide in cells renders them resistant to HIV infection because of a block in membrane fusion. Notably, the importance of ceramide in inhibiting HIV-1 infection in primary cells has been shown, highlighting a possible novel target for antiretroviral therapy.

Experimental Procedures

Reagents and Cells. The TZM-bl indicator cell line (7), obtained through the AIDS Research and Reference Reagent Program, Division of AIDS, National Institute of Allergy and Infectious Diseases, National Institutes of Health, from J. C. Kappes, X. Wu, and Tranzyme (Research Triangle Park, NC), is a HeLa cell line derivative that expresses high levels of CD4 and CCR5 along with endogenously expressed CXCR4. TZM-bl cells contain HIV LTR-driven β-galactosidase and luciferase reporter cassettes that are activated by HIV Tat expression. Cells are routinely subcultured every 3 to 4 days by trypsinization and are maintained in DMEM supplemented with 10% FBS and 1× penicillin–streptomycin (complete media) at 37°C with 5% CO_2 in a humidified incubator. Sphingomyelinase (Smase) derived from *Bacillus cereus*, etoposide, and daunorubicin were obtained from Sigma. *N*-(4-hydroxyphenyl)retinamide (4-HPR) was purchased from Biomol (Plymouth Meeting, PA). Lipids were obtained from Avanti Polar Lipids.

Infectivity Assay. TZM-bl cells (2×10^4 per well) were added to 96-well microtiter plate (Falcon) in 100 μl of complete media and allowed to adhere 15–18 h at 37°C. In assays where pretreatments were used, TZM-bl cells were plated at 0.75×10^4 cells per well in a 96-well plate and treated with various concentrations of 4-HPR, etoposide, or daunorubicin for 48 h. An equivalent amount of each virus stock (a multiplicity of infection of 0.01) was added to the cell monolayers in the presence of 40 μg/ml DEAE-dextran in DMEM in a final volume of 100 μl. Viral infection was allowed to proceed for 2 h at 37°C after which 100 μl of complete DMEM media was added. Luciferase activity was measured after 15–18 h by using a Promega luciferase assay system kit. The light intensity of each well was measured on a reporter luminometer. Mock-infected cells were used to determine background luminescence. All infectivity assays were performed in duplicate.

Smase Treatment and Exogenous Ceramide Addition. To induce cell-surface ceramide, cells were incubated with purified Smase at 50 milliunits/ml, unless otherwise stated, for 10 min at 37°C. For exogenous lipid addition, 1 mM C16 ceramide, brain ceramide, or the control lipids 1,2-dipalmitoyl-*sn*-glycerol, 1,2-dioleoyl-*sn*-glycerol, and sphingomyelin were sonicated for 5 min in ethyl alcohol. Ten microliters of this solution was dissolved in 90 μl of Diluent C (Sigma) and sonicated for 5 min, yielding a stock solution of 100 μM lipid. Cells were then treated for 30 min with each lipid solution at a final concentration of 1 μM in DMEM.

This paper was submitted directly (Track II) to the PNAS office.

Abbreviations: 4-HPR, *N*-(4-hydroxyphenyl)retinamide; Smase, sphingomyelinase; MDM, monocyte-derived macrophage; BlaM, β-lactamase.

§To whom correspondence should be addressed at: P.O. Box B, Building 469, Room 216A, Miller Drive, Frederick, MD 21702-1201. E-mail: blumen@helix.nih.gov.

Ceramide Quantitation. Cells were incubated with 1 μCi (1 Ci = 37 GBq) [^{3}H]sphingosine (specific activity 20 Ci/mmol; American Radiological Chemicals, St. Louis) in medium containing 4-HPR, daunorubicin, or etoposide at the indicated final concentrations for 48 h. For Smase treatment, cells labeled for 48 h with [^{3}H]sphingosine were incubated with 50 milliunits/ml of *Bacillus cereus* Smase (Sigma) and incubated for 10 min at 37°C. Lipids were then extracted according to Bligh and Dyer (8). The extracted lipid phase was pooled, dried under N_2, and resuspended in $CH_3OH/CHCl_3$ (2:1 ratio, vol/vol). A small amount of the extract from each treatment was used for normalization. After normalization, the lipid extracts labeled with [^{3}H]sphingosine were run on TLC plates. The TLC was developed in solvent system comprised of $CHCl_3/CH_3OH/H_2O$ (65:25:4 ratio, vol/vol/vol). The TLC plates were then sprayed lightly with En^{3}hance (PerkinElmer), and radioactive lipids were visualized by autoradiography after 48 h at −80°C. The radioactive spot migrating with the ceramide standard was scraped from the plate and quantified by liquid scintillation spectrometry.

HIV Infectivity of Primary Cells. Leukopaks of peripheral blood were collected from adult donors by the National Institutes of Health Transfusion Branch (Bethesda) according to the approved National Institutes of Health Institutional Review Board Protocols. Mononuclear cells were isolated by Ficoll/Hypaque gradient centrifugation (Sigma-Aldrich, St. Louis). T cells and monocytes were separated by countercurrent elutriation. CD4$^+$ T cells were then isolated by negative selection using magnetic-activated cell-sorting methods according to the manufacturer's instructions (Miltenyi Biotec, Sunnyvale, CA). The CD4$^+$ lymphocyte populations were consistently >95% pure. After isolation, the cells were cultured in RPMI medium 1640 supplemented with 10% FCS, 2 mM L-glutamine, 1 nM sodium pyruvate, antibiotics, and 20 units/ml recombinant human IL-2 (PeproTech, Rocky Hill, NJ), and activated with 1 μg/ml phytohemagglutinin. Purified monocytes were cultured in RPMI medium 1640 containing 5% human AB sera in six-well plates. After day 5 of culture, both T cells and monocytes were incubated with the indicated concentrations of 4-HPR for 48 h. In some experiments, Smase was added to the T cells for 1 h at 200 milliunits/ml and to monocyte-derived macrophages (MDMs) for 15 min at 50 milliunits/ml immediately before infection.

Activated CD4$^+$ PBMCs (5×10^6) and monocytes were infected with a multiplicity of infection of 0.1 (≈100 pg of HIV p24 per ml). After a 90-min absorption period at 37°C, cells were washed with PBS and fresh growth media were added. Cells were then cultured at 5×10^5 cells per ml for 3–14 days and cells were fed every 4 days. HIV-1 p24 levels were measured on frozen cell-free supernatant at various times by using an ELISA kit (Zeptometrix, Buffalo, NY) according to the instructions. The minimal level of p24 detection was 7 pg/ml.

Chemotaxis Assay. Chemotaxis assays for human CD4$^+$ T cells and macrophages were performed with 48-well chemotaxis chambers (Neuroprobe, Gaithersburg, MD). Different concentrations of chemokines were placed in wells of the lower compartment of the chamber. The cell suspension (1×10^6 per ml in RPMI medium 1640, 1% BSA) was seeded into wells of the upper compartment, which was separated from the lower compartment by polycarbonate filters (GE Osmonics Labstore, Minnetonka, MN; 5-μM pore size for macrophages and 3-μM pore size for T cells). The filters for migration of T cells were precoated with 10 ng/ml fibronectin (Collaborative Biomedical Products, Bedford, MA). After incubating the chemotaxis chambers at 37°C (90 min for macrophages and 180 min for T cells), the filters were removed and stained, and the numbers of cells migrating across the filters were counted by light microscopy after coding the samples. Results are presented as the chemotaxis indexes representing the fold increase in the number of migrating cells in response to stimuli over the spontaneous cell migration (to control medium).

β-Lactamase (BlaM) Virion-Based Fusion Assay. The virion-based fusion assay was performed as described (9) with minor modifications. TZM-bl cells were plated on a 96-well plate at a density of 0.75×10^4 cells per well and incubated with various concentrations of 4-HPR for 48 h. In some experiments, Smase was added to the TZM-bl cells for 10 min at 50 milliunits/ml immediately before infection. Fifty microliters of virus containing supernatant and 50 μl of DMEM containing 80 μg/ml DEAE-dextran was then added to each well, and infection was allowed to proceed for 2 h at 37°C. The cells were then washed in CO_2-independent media and loaded with CCF2/AM dye as described by the manufacturer (Invitrogen). Cells were incubated in the loading solution for 1 h at room temperature. The loading solution was then removed, and the cells were washed twice with CO_2-independent media. The BlaM reaction was allowed to develop for 12 h at room temperature in 200 μl of CO_2-independent media supplemented with 2.5 mM probenecid, a nonspecific anion transport inhibitor. Digital images were collected by using an Olympus 1 × 70 microscope (Melville, NY) equipped with a CCF2 filter set (Chroma Technology, Brattleboro, VT). Images were processed with METAMORPH V4.0 software (Universal Imaging, West Chester, PA).

Results

Pharmacological Stimulation of Ceramide Synthesis Inhibits HIV-1 Infection. The use of 4-HPR, a synthetic derivative of retinoic acid, specifically increases the generation of *de novo* ceramide through the activation of two key enzymes in the ceramide synthesis pathway, serine palmitoyltransferase and ceramide synthase (10). To test its effects on HIV-1 entry, we used the indicator cell line, TZM-bl, which is susceptible to infection by diverse HIV isolates. After viral fusion, the LTR-driven reporter gene products luciferase and β-galactosidase are expressed, allowing for quantitative measurement of viral infectivity as soon as 16 h after infection. Fig. 1 shows a dose-dependent inhibition of infection by HIV-1 isolates that use CXCR4 (NL4-3 and MN) (Fig. 1*A*), CCR5 (Ba-L, JRCSF, and 92US727) (Fig. 1*B*), or by dual-tropic primary HIV-1 isolates (Fig. 1*C*). In contrast to the potent inhibitory effect of 4-HPR on HIV-1, infectivity of vesicular stomatitis virus pseudotyped HIV-1 was not impaired under similar 4-HPR concentrations (data not shown). Therefore, such inhibition appears to be specific for HIV-1 envelope-mediated fusion. Notably, inhibition of HIV-1 is observed at low micromolar concentrations for 4-HPR with an IC_{50} of <1 μM for most isolates tested. There was considerable variability in IC_{50} and maximal inhibition between the different isolates (Table 1). Whether the sensitivity/resistance of these HIV-1 isolates to 4-HPR correlates with envelope coreceptor affinity, fusion kinetics, or other factors still needs to be determined. However, it does not appear that laboratory-adapted isolates, which are generally more neutralization-sensitive, are more susceptible to inhibition by 4-HPR. As seen in Table 1, the IC_{50} values of primary isolates were as low as 0.047 μM for HIV-$1_{92US077}$ (Table 1).

To relate the mode of action of 4-HPR to changes in ceramide, we determined ceramide levels after metabolic incorporation of [^{3}H]sphingosine for 48 h in the absence and the presence of different concentrations of 4-HPR. Fig. 1*D* shows a linear increase in ceramide levels at 4-HPR concentrations up to 10 μM. However, the assay is not sufficiently sensitive to measure changes at low 4-HPR concentrations. Extrapolating to 1 μM 4-HPR, a concentration at which nearly maximal inhibition was seen for most isolates, yields a 20% increase in ceramide levels.

We tested two additional agents that affect ceramide levels of cells: etoposide, an activator of serine palmitoyltransferase (11),

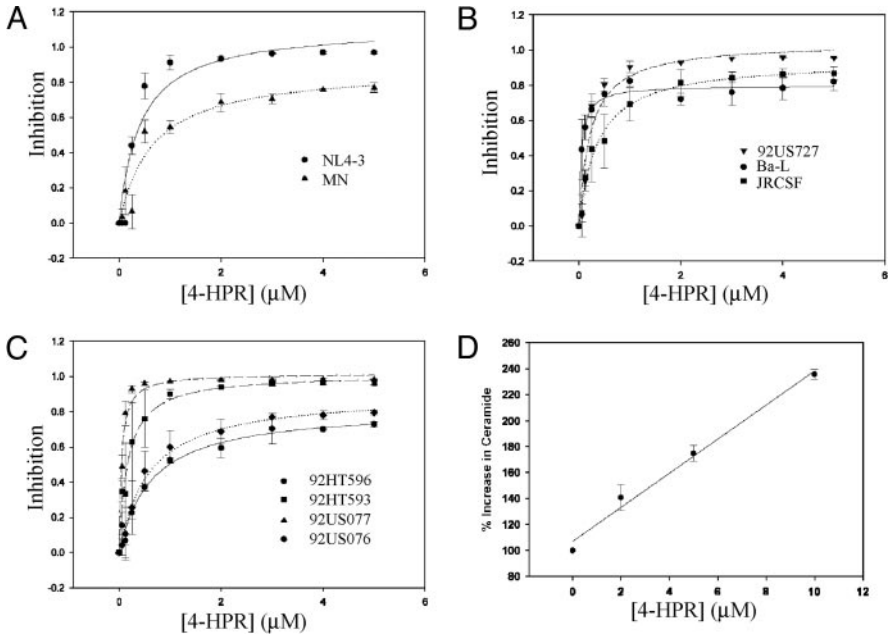

Fig. 1. The use of 4-HPR enhances ceramide levels in TZM-bl cells and blocks HIV-1 infectivity. TZM-bl cells were incubated with 4-HPR for 48 h at 37°C. HIV-1 infection was carried out as described in *Experimental Procedures* by using the indicated HIV-1 isolate at a multiplicity of infection of 0.01. Luciferase activity was quantified after 16 h, and viral inhibition was calculated relative to control untreated cells. Data are representative of an assay performed in duplicate and are representative of three independent experiments giving similar results. The lines represent best fits to a simple hyperbolic function by using the program SIGMAPLOT. (*A*) CXCR4 isolates. (*B*) CCR5 isolates. (*C*) Dual-tropic primary isolates. (*D*) Measurement of the increase in TZM-bl ceramide levels after 4-HPR treatment by using the [^{3}H]sphingosine incorporation method described in *Experimental Procedures*.

and daunorubicin, an activator of ceramide synthase (12). Table 2 shows that ceramide levels of TZM-bl cells treated with these agents are enhanced by 40–70% at concentrations where maximal inhibition was observed. Table 2 also shows that the IC_{50} values for inhibition of entry by HIV-1_{NL4-3} were in the 0.1–0.2 μM range. We also measured cell killing mediated by these agents. TC_{50}, the concentration of the drug that elicits cytotoxicity in 50% of uninfected cells, was 10- to 100-fold higher for 4-HPR and etoposide, whereas daunorubicin had a TC_{50} value only 3 times higher than its IC_{50} for inhibition of HIV-1 infection. These data show that the therapeutic indices for 4-HPR and etoposide, but not daunorubicin, would be appropriate for treatment of infected individuals.

In addition to *de novo* synthesis, ceramide can also be formed through the enzymatic catabolism of sphingomyelin. Sphingomyelin is mainly located on the outer leaflet of the plasma membrane and the addition of Smase C specifically catabolizes sphingomyelin into ceramide. To determine whether such enzymatic generation of ceramide directly at the plasma membrane could inhibit HIV-1 infection, we pretreated cells for 10 min at 37°C with Smase C. In accordance with the specificity of this enzyme, we determined through metabolic incorporation of [^{3}H]sphingosine that ceramide levels were increased by 164% (data not shown) after this treatment. HIV-1_{NL4-3} was then added and infection was allowed to proceed as described. Under these conditions where ceramide is enzymatically generated, infection of TZM-bl cells by HIV-1_{NL4-3} was inhibited by 75% (Table 3).

To further confirm that ceramide accumulation at the plasma membrane inhibits HIV-1 infection, we added exogenous ceramide directly to target cells before infection. We selected saturated acyl chain ceramides, either synthetic C16 ceramide or porcine brain ceramide (predominantly composed of C18, with

Table 1. Inhibition of HIV-1 entry by 4-HPR

Isolate	Maximum inhibition, μM	IC_{50},* μM
NL4-3	1.12	0.13
MN	0.88	0.65
Ba-L	0.80	0.05
JRCSF	0.94	0.36
92US727	1.04	0.22
92HT593	1.01	0.17
92US077	1.02	0.047
92HT596	0.82	0.63
92US076	0.90	0.58

*HIV-1 entry in TZM-bl cells was measured using the luciferase reporter gene assay described in the Fig. 1 legend. IC_{50}, the concentration of antiviral drug that reduced the infection levels by 50% in comparison with the infected, untreated control, and maximal inhibition (at high concentrations of 4-HPR), was determined by fitting the dose–response curves to a simple hyperbolic function by using the program SIGMAPLOT (SPSS, Chicago).

Table 2. Inhibition of HIV-1 entry by pharmacological agents

Agent	Percent increase in ceramide*	IC_{50},† μM	TC_{50},‡ μM
4-HPR	70 (5 μM)	0.13	12.5
Daunorubicin	40 (250 nM)	0.11	0.31
Etoposide	50 (10 μM)	0.24	17.4

*The percent increase is 100 (ceramide levels in treated cells)/(ceramide levels in untreated cells). The ceramide determinations were carried out at the concentrations of the pharmacological agent indicated by the numbers in parentheses.

†HIV-1_{NL4-3} entry in TZM-bl cells was measured using the luciferase reporter gene assay described in the Fig. 1 legend. IC_{50}, the concentration of antiviral drug that reduced the infection levels by 50% in comparison with the infected, untreated control, was determined by fitting the dose–response curves to a simple hyperbolic function by using the program SIGMAPLOT.

‡TC_{50} is the concentration of the drug that elicits cytotoxicity in 50% of uninfected cells.

Table 3. Inhibition of HIV-1 entry by Smase and exogenous lipid addition

Agent	Percent inhibition
Smase C	75
Ceramide (C16)	60
Brain ceramide (C18)	65
1,2-dipalmitoyl-*sn*-glycerol (C16)	13
1,2-dioleoyl-*sn*-glycerol (C18)	3
Sphingomyelin	5

HIV-1_{NL4-3} entry in TZM-bl cells was measured by using the luciferase reporter gene assay described in the Fig. 1 legend.

minor species of C16, C20, C22, and C24). Such long-chain ceramides most likely mimic the hydrophobic and partitioning properties of endogenous ceramide. Pretreatment of target cells with 1 μM ceramide for 30 min at 37°C resulted in inhibition of HIV infection (Table 3). In contrast, the addition of control lipids, 1,2-dipalmitoyl-*sn*-glycerol, a saturated C16 lipid, 1,2-dioleoyl-*sn*-glycerol, an unsaturated C18 lipid, or sphingomyelin did not result in inhibition of HIV-1 infection. These results confirm our previous findings that increasing ceramide inhibits HIV-1 infection (Fig. 1). Moreover, taken together with the inhibitory activity observed after Smase treatment, these findings strongly implicate cell-surface ceramide in mediating this inhibition.

The Use of 4-HPR Inhibits HIV-1 Infection in Primary CD4$^+$ T Cells and Macrophages. Having established that 4-HPR has inhibitory consequences for viral infection in an epithelial carcinoma cell line (HeLa), we next determined the effects of such perturbation on HIV-1 infection of primary CD4$^+$ T cells and MDMs. As shown in Fig. 2*A*, treatment of CD4$^+$ T cells with 4-HPR results in a dose-dependent inhibition of HIV-1 infection as measured by p24 antigen release. Sixty percent inhibition of the primary isolate HIV-$1_{92US727}$ is observed in CD4$^+$ T cells after treatment with 1 μM 4-HPR, whereas 10 μM 4-HPR treatment results in 80% inhibition of viral infection. In agreement, analysis of the percentage of cells infected by intracellular viral core staining also demonstrates a significant reduction. Untreated CD4$^+$ T cells when stained with a specific HIV-1 core antibody result in 58% of the cell population staining positive for infection (Fig. 2*B*). The use of 4-HPR treatment decreases the population of infected cells to 15% and 3% after 1 and 10 μM 4-HPR treatment, respectively.

We also investigated the effect of 4-HPR on HIV-1 infection of MDM because MDM play an important role in HIV pathogenesis. As for CD4$^+$ T cells, 4-HPR at 1 and 10 μM reduced HIV infectivity as detected by extracellular p24 (Fig. 2*C*) and intracellular HIV core staining (Fig. 2*D*). Treatment of MDM with 10 μM 4-HPR resulted in a log reduction of p24 production after 7 days by HIV-$1_{92US727}$ (Fig. 2*C*). The inhibition of infection of MDMs by HIV-1_{Ba-L} was somewhat less, as was the case in TZM-bl cells. In agreement, when the number of infected cells was measured by intracellular core staining, a large reduction was observed after treatment of MDMs with 4-HPR (Fig. 2*D*). Pretreatment of MDMs with 10 μM 4-HPR decreased the number of HIV-1-positive cells from 72% infected to 3% infected for the primary isolate HIV-$1_{92US727}$ and from 64% infected to 6% infected for HIV-$1_{Ba-L.}$ Ceramide levels in CD4$^+$ lymphocytes and MDMs were slightly enhanced after treatment with 2 μM 4-HPR and ≈50–80% enhanced at 5 and 10 μM 4-HPR, respectively (data not shown).

To further confirm that increasing ceramide levels in primary cells contributed to an inhibition to HIV-1 infection, we pretreated CD4$^+$ T cells and MDMs with Smase C. Such pretreatment resulted in a 112% and 157% elevation in ceramide levels

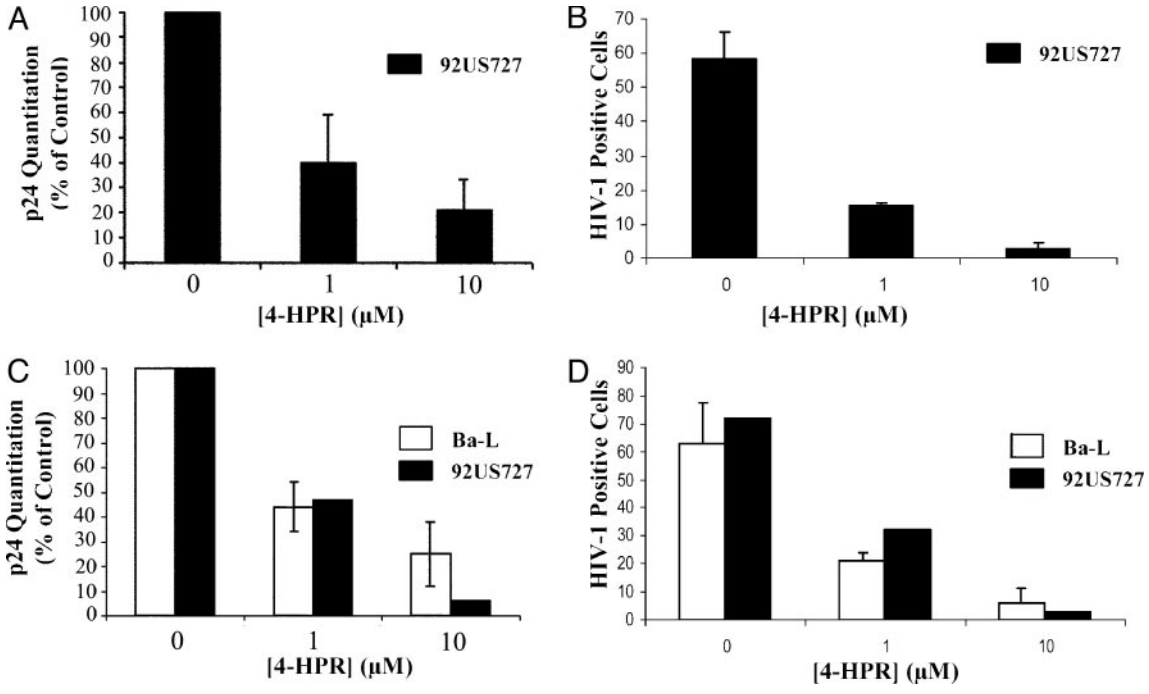

Fig. 2. Effect of HPR on HIV-1 infectivity in CD4$^+$ T cells and MDMs. (*A* and *B*) Activated CD4$^+$ T cells were treated for 48 h with 4-HPR at the indicated concentration and then infected with HIV-$1_{92US727}$. Infectivity was determined by p24 production (*A*) and by intracellular viral core staining (*B*) after 7–12 days as described in *Experimental Procedures*. Data are representative of three independent experiments. (*C* and *D*) Elutriated monocytes were differentiated for 5 days and incubated with 4-HPR for 48 h as described in *Experimental Procedures*. Infectivity was determined after infection with HIV-1_{Ba-L} or HIV-$1_{92US727}$ by p24 production (*C*) and by intracellular viral core staining (*D*). Data are representative of three independent experiments for HIV-1_{Ba-L} infectivity and of one experiment for HIV-$1_{92US727}$ infectivity.

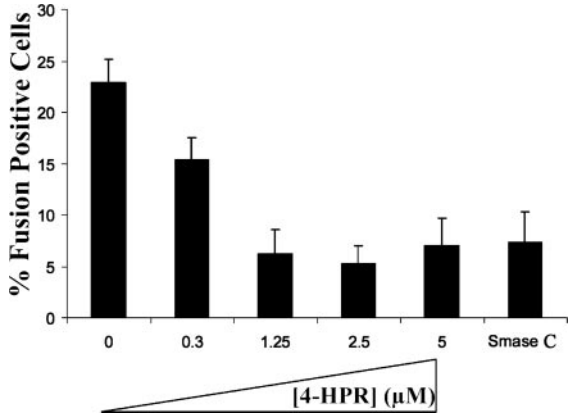

Fig. 3. The use of 4-HPR inhibits viral cell fusion. Target cells were treated with 4-HPR at the indicated concentration for 48 h before the fusion assay. Infection was then carried out for 2 h by using HIV-1 BlaM virions as described in *Experimental Procedures*. After infection, target cells were loaded with CCF2/AM dye for 1 h, and the BlaM reaction was allowed to proceed for 12 h at room temperature. The percentage of infected cells (number of blue cells per 100 cells) was calculated for 4-HPR-treated untreated target cells and Smase C-treated cells. The results represent an average of two independent experiments. The total number of cells counted for each condition are as follows: Control, 2,208; 0.3 μM 4-HPR, 792; 1.25 μM 4-HPR, 1,857; 2.5 μM 4-HPR, 1,446; 5 μM 4-HPR, 1,540; and Smase, 1,929.

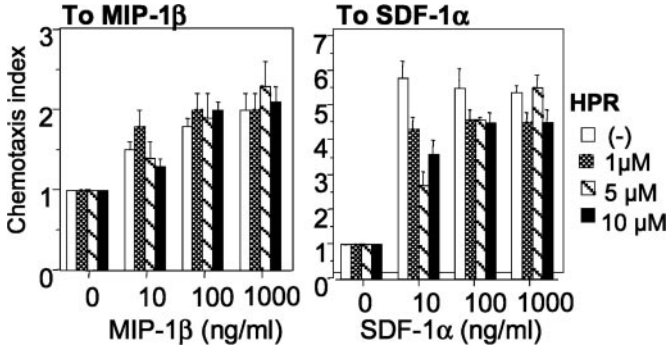

Fig. 4. Chemokine-triggered cell migration. Different concentrations of SDF-1α (*Right*) or MIP1-β (*Left*) were placed in the lower wells of the chemotaxis chamber. CD4$^+$ T cells were treated for 2 days with 4-HPR at the indicated concentrations and placed in the upper wells, which were separated from the lower wells by a polycarbonate filter. The results are expressed as chemotaxis index representing the fold increase of migrating cells in response to chemokines over the response to control medium. Significant cell migration ($P < 0.05$) was detected with 10 ng/ml chemoattractant.

for CD4$^+$ T cells and MDMs, respectively. Pretreatment of CD4$^+$ T cells with Smase C resulted in 68% inhibition of HIV-1 infection as determined from p24 antigen release, whereas similar treatment of MDMs inhibited HIV-1 infection by 76% (data not shown). This result is consistent with the notion that the inhibitory effect of 4-HPR on HIV-1 infection of primary CD4$^+$ T cells and MDMs is primarily due to changes in ceramide levels in these cells.

The Use of 4-HPR Inhibits Viral Fusion. To examine whether the inhibitory effect of 4-HPR is due to inhibition of virus cell fusion, we performed the BlaM virion-based direct-fusion assay that detects infection due to the activity of virion-associated BlaM (9). This enzyme is incorporated into virions due to association with the viral protein Vpr. Once released into the cytoplasm of infected cells, BlaM can cleave CCF2/AM, a fluorescent substrate that is loaded into target cells. Cleavage of this substrate changes the emission spectrum of the dye from green (520 nm) to blue (447 nm), allowing infected cells to be visualized (9). Counting the number of blue cells in the population allows for a quantitative analysis of viral fusion. As seen in Fig. 3, 4-HPR treatment of TZM-bl cells resulted in significant inhibition of viral fusion. In untreated control cells, 23% of the cell population were positive for viral fusion, whereas 4-HPR treatment at concentrations of 1.25 to 5 μM decreased this number to 5–7%. Hence, viral fusion as determined in this assay system was inhibited 70–78%. As expected, at lower concentrations of 4-HPR, this inhibitory effect was diminished with 15% of the cell population scoring positive for fusion (35% inhibition). We also quantitated the effect of Smase C pretreatment on viral fusion. In agreement with the inhibition observed after 4-HPR treatment, 7% of the cell population scored positive for fusion, indicating a 70% inhibitory effect. These results indicate that the inhibitory effect of 4-HPR is predominantly due to inhibition of viral cell fusion.

One hypothesis to explain this inhibition is that chemokine receptor expression or function is altered. Hence, we investigated the expression of the HIV receptors, CD4, CXCR4, and CCR5 on CD4$^+$ T lymphocytes and MDMs after 4-HPR treatment. At low micromolar concentrations of 4-HPR, which result in significant fusion inhibition for most isolates tested (Fig. 1 and Table 1), little down-regulation of CD4, R5, or X4 levels was observed (data not shown). We also tested the conformation and function of the coreceptors, by examining migration of cells in response to the CXCR4 agonist SDF-1α and the CCR5 agonist MIP-1β. Treatment of CD4$^+$ T cells with concentrations of 4-HPR that significantly reduced infectivity had little effect on chemotaxis (Fig. 4). Therefore, the inhibition of HIV-1 infection cannot be attributed to possible changes in chemokine receptor expression or function.

Discussion

In this study, we demonstrate that increasing cellular ceramide levels inhibits HIV-1 infection. This effect can be mediated by pharmacological stimulation of ceramide biosynthesis (Figs. 1–3 and Tables 1 and 2), through the action of Smase at the cell surface (Table 3), or through the addition of exogenous long-chain ceramide (C16 or C18) (Table 3). Evidence from viral fusion experiments indicates that mechanistically such inhibition likely occurs at the level of membrane fusion (Fig. 3). The reduced susceptibility cannot be attributed to a reduction in HIV receptor levels or altered conformation as indicated by the chemotaxis experiments (Fig. 4).

CD4 appears to be localized in cholesterol and glycosphingolipid-enriched membrane microdomains (rafts) (13). Experimental results suggest that integrity of lipid rafts is important for HIV-1 entry, and destabilizing rafts by extraction of cholesterol inhibits HIV-1 entry (14–19). However, studies with CD4 mutants that do not partition into rafts yielded conflicting results, which indicate that localization of CD4 in rafts is essential (20), or nonessential (21, 22), for HIV-1 entry. Other studies indicate that membrane cholesterol is required to maintain chemokine receptor conformation that allows engagement of HIV-1 Env (19, 23, 24).

We hypothesize that the increase in plasma membrane ceramide levels affects HIV-1 entry by perturbing localized membrane domain structure and organization (5). Upon HIV-1 engagement of CD4, as the pool of coreceptors reside in a phase-separated domain; infectivity is reduced due to the low probability of coreceptor engagement. This perturbation of membrane structure may result in the trafficking of virions via an endocytic pathway that leads to nonproductive infection (25). Future studies are warranted to test this hypothesis. Very low ceramide concentrations are required to induce membrane lateral phase separations (26, 27). This outcome is consistent

with our observation that minor changes in cellular ceramide levels result in the inhibition of HIV-1 entry. In contrast to perturbing membrane structure as a result of cholesterol removal, these small changes in ceramide levels do not appear to affect chemokine receptor conformation and function (see Fig. 4).

The inhibitory effects of ceramide accumulation in HIV infection are important for several reasons. First, infection was inhibited at pharmacologically achievable concentrations of 4-HPR (28), a drug that has shown very low toxicity in clinical trials and is approved for chemotherapeutic use. Because such chemotherapy drugs function by increasing ceramide, a key mediator of the apoptotic response, a high therapeutic index is critical when considering the potential applications of these drugs to antiviral therapy. As observed in Table 2, the TC_{50} for 4-HPR greatly exceeds the IC_{50}, indicating that this drug has a high therapeutic index and would not be expected to trigger significant apoptosis *in vivo*. On a cautionary note, it is possible that HIV-infected individuals that already have perturbed sphingolipid metabolism, as is observed in HIV dementia, may not tolerate drugs that stimulate ceramide biosynthesis. Further studies are needed to investigate the effects of this approach on infected individuals. It is also noteworthy that although the IC_{50} of 4-HPR for all isolates tested was <1 μM, complete inhibition was not observed for some isolates. Future investigation of the possibility that there is a heterogenous response in the cell population to 4-HPR stimulation, perhaps with a subpopulation of cells being refractory at the concentrations tested, is warranted. We anticipate that 4-HPR would be used in combination with current antiviral regiments *in vivo* to achieve maximal inhibition and prevent the outgrowth of resistant viruses. Second, this study identifies a target for antiretroviral therapy, ceramide biosynthesis, which can be further exploited for the development of antiviral agents. Third, further studies to elucidate the mechanism of action resulting in viral inhibition could likely lead to the development of novel targets for HIV therapy.

We thank Warner Greene (Gladstone Institute of Virology and Immunology, San Francisco) for his gift of pCMV-BlaM-Vpr; Himanshu Garg for generating the BlaM-containing virions and for technical assistance with the BlaM fusion assay; Wanghua Gong for expert technical assistance with the chemotaxis experiments; Cari Sadowski for expert technical assistance with the primary cell infectivity assays; and the AIDS Research and Reference Reagent Program for the contribution of reagents that were used in this study. This work was supported by the AIDS Targeted Antiviral Program of the Office of the Director of the National Institutes of Health.

1. Gallo, S. A., Finnegan, C. M., Viard, M., Raviv, Y., Dimitrov, A., Rawat, S. S., Puri, A., Durell, S. & Blumenthal, R. (2003) *Biochim. Biophys. Acta* **1614,** 36–50.
2. Singer, I. I., Scott, S., Kawka, D. W., Chin, J., Daugherty, B. L., DeMartino, J. A., DiSalvo, J., Gould, S. L., Lineberger, J. E., Malkowitz, L., *et al.* (2001) *J. Virol.* **75,** 3779–3790.
3. Rawat, S. S., Viard, M., Gallo, S. A., Rein, A., Blumenthal, R. & Puri, A. (2003) *Mol. Membr. Biol.* **20,** 243–254.
4. Hannun, Y. A. & Obeid, L. M. (2002) *J. Biol. Chem.* **277,** 25847–25850.
5. Cremesti, A. E., Goni, F. M. & Kolesnick, R. (2002) *FEBS Lett.* **531,** 47–53.
6. Grassme, H., Jendrossek, V., Riehle, A., Von Kurthy, G., Berger, J., Schwarz, H., Weller, M., Kolesnick, R. & Gulbins, E. (2003) *Nat. Med.* **9,** 322–330.
7. Wei, X., Decker, J. M., Liu, H., Zhang, Z., Arani, R. B., Kilby, J. M., Saag, M. S., Wu, X., Shaw, G. M. & Kappes, J. C. (2002) *Antimicrob. Agents Chemother.* **46,** 1896–1905.
8. Bligh, E. G. & Dyer, W. J. (1959) *Can. J. Biochem. Physiol.* **37,** 911–917.
9. Cavrois, M., De Noronha, C. & Greene, W. C. (2002) *Nat. Biotechnol.* **20,** 1151–1154.
10. Wang, H., Maurer, B. J., Reynolds, C. P. & Cabot, M. C. (2001) *Cancer Res.* **61,** 5102–5105.
11. Perry, D. K., Carton, J., Shah, A. K., Meredith, F., Uhlinger, D. J. & Hannun, Y. A. (2000) *J. Biol. Chem.* **275,** 9078–9084.
12. Bose, R., Verheij, M., Haimovitz-Friedman, A., Scotto, K., Fuks, Z. & Kolesnick, R. (1995) *Cell* **82,** 405–414.
13. Sorice, M., Parolini, I., Sansolini, T., Garofalo, T., Dolo, V., Sargiacomo, M., Tai, T., Peschle, C., Torrisi, M. R. & Pavan, A. (1997) *J. Lipid Res.* **38,** 969–980.
14. Manes, S., del Real, G., Lacalle, R. A., Lucas, P., Gomez-Mouton, C., Sánchez-Palomino, P., Delgado, R., Alcamí, J., Mira, E. & Martinez-A., C. (2000) *EMBO Rep.* **1,** 190–196.
15. Liao, Z., Cimakasky, L. M., Hampton, R., Nguyen, D. H. & Hildreth, J. E. (2001) *AIDS Res. Hum. Retroviruses* **17,** 1009–1019.
16. Campbell, S. M., Crowe, S. M. & Mak, J. (2001) *J. Clin. Virol.* **22,** 217–227.
17. Viard, M., Parolini, I., Sargiacomo, M., Fecchi, K., Ramoni, C., Ablan, S., Ruscetti, F. W., Wang, J. M. & Blumenthal, R. (2002) *J. Virol.* **76,** 11584–11595.
18. Kozak, S. L., Heard, J. M. & Kabat, D. (2002) *J. Virol.* **76,** 1802–1815.
19. Nguyen, D. H. & Taub, D. (2002) *J. Immunol.* **168,** 4121–4126.
20. Del Real, G., Jimenez-Baranda, S., Lacalle, R. A., Mira, E., Lucas, P., Gomez-Mouton, C., Carrera, A. C., Martinez, A. & Manes, S. (2002) *J. Exp. Med.* **196,** 293–301.
21. Percherancier, Y., Lagane, B., Planchenault, T., Staropoli, I., Altmeyer, R., Virelizier, J. L., Arenzana-Seisdedos, F., Hoessli, D. C. & Bachelerie, F. (2003) *J. Biol. Chem.* **278,** 3153–3161.
22. Popik, W. & Alce, T. M. (2003) *J. Biol. Chem.* **279,** 704–712.
23. Nguyen, D. H. & Taub, D. (2002) *Blood* **99,** 4298–4306.
24. Nguyen, D. H. & Taub, D. D. (2003) *Exp. Cell Res.* **291,** 36–45.
25. Schaeffer, E., Soros, V. B. & Greene, W. C. (2004) *J. Virol.* **78,** 1375–1383.
26. Veiga, M. P., Arrondo, J. L., Goni, F. M. & Alonso, A. (1999) *Biophys. J.* **76,** 342–350.
27. Carrer, D. C. & Maggio, B. (1999) *J. Lipid Res.* **40,** 1978–1989.
28. Formelli, F. & Cleris, L. (1993) *Cancer Res.* **53,** 5374–5376.